Resonator-qutrit quantum battery

Fang-Mei Yang and Fu-Quan Dou*
College of Physics and Electronic Engineering, Northwest Normal University, Lanzhou 730070, China

(Received 19 March 2024; accepted 29 May 2024; published 24 June 2024)

Quantum batteries (QBs) are energy storage and transfer microdevices that open up new possibilities in energy technology. Here, we derive a resonator–multiple-qutrit quantum battery (QB) model consisting of a multimode resonator and N superconducting transmon qutrits. We investigate the charging and self-discharging performances of the QBs and discuss the roles of quantum coherence and quantum entanglement. The results show that environment noise is not always detrimental for QB systems. The QB with efficient charging, stable energy-storage, and slow self-discharging processes can be realized by considering the dephasing noise and manipulating the energy gap. We find that the charging energy is positively related to coherence and entanglement while the stable energy and the self-discharging energy are negatively related to coherence. The phenomenon of the vanishing entanglement corresponds to the dynamic decoupling behavior of the QB's steady states. Our results provide a way to realize many-body QBs on a superconducting circuit platform.

DOI: 10.1103/PhysRevA.109.062432

I. INTRODUCTION

Motivated by the ongoing miniaturization of electronic equipment and the rapid development of quantum thermodynamics in micro- and mesoscopic quantum systems, Alicki and Fannes introduced the notion of quantum battery (QB) to temporarily store energy and suggested that entangling unitary operations can extract more work than local ones [1]. Subsequently, it was shown that some protocols exist for optimal work extraction actually without creating any entanglement, at the cost of generically requiring more operations [2,3]. Further research uncovered that entanglement may have a disruptive effect on the performance of quantum batteries (QBs) [4–7], whereas coherence appears to be a potential resource [7–14]. In recent years, how to exploit quantum resources like entanglement and coherence to outperform their classical counterpart has been a major focus in the quantum thermodynamics realm, but the couplings among different quantum resources have made the problem intractable and complicated [7,15–22].

Nowadays, the development of QBs is still in its infancy and there are many challenges that need to be adequately solved before such quantum devices can be implemented in practice. Besides the wide concerns of efficient charging [22–42] and stable energy-storage processes [16,43–54], it is also important to highlight the self-discharging process characterized by the decay of energy when no consumption hubs are connected to QBs. How to manage the undesired effects and boost the ability of QBs to store energy during the self-discharging process is a key task [54–58]. At present, some protocols have been proposed to preserve the energy stored in QBs for long times, e.g., considering spectrum engineering [54,55] and non-Markovian effects [56], introducing local field fluctuation described by the disorder term in the system Hamiltonian [57], and manipulating coherence of the initial states and geometry of the intracell connections [58].

Experimentally, several studies have exhibited some advantages of QBs. The realization of a QB utilizing an organic semiconductor as an ensemble of two-level systems coupled to a microcavity showed that the power density of a Dicke QB is up to 672 kW/kg, which far exceeds the power densities of existing lithium-ion batteries [59,60]. Up to now, QBs have been promisingly implemented on many physical platforms [60–71], including organic semiconductor [60] and semiconductor quantum dots [66] coupled to optical microcavities, nuclear spin systems with a star-topology configuration [65], photonic systems using polarizations of single photons [67,68], and superconducting circuits systems operating at millikelvin temperatures [69–71]. Compared to other platforms, superconducting circuits are of great interest because of their flexibility, adjustability, scalability, and strong coupling with external fields [72–76]. In 2019, Santos *et al.* proposed that superconducting circuits are an effective platform on which to realize QBs [54] and the viewpoint has been confirmed in subsequent experiments which generally consist of one superconducting qutrit driven by classical fields [64,69–71]. Remarkably, the semiclassical QB model designed on superconducting circuits can ensure a stable charged state by using the stimulated Raman adiabatic passage, but has limited charging energy and fast self-discharging speed. Therefore, the exploration of many-body QBs with efficient charging, stable energy-storage, and slow self-discharging processes on a superconducting circuit platform is necessary and meaningful.

In this paper, we focus on a superconducting circuit system composed by a one-dimensional transmission line resonator and N coupled transmons. Under the condition that the anharmonicity of the transmon is smaller than the transmon-resonator detuning, we derive the general Hamiltonian of

*Contact author: doufq@nwnu.edu.cn

this superconducting circuit system and define three QBs, including the one-mode or two-mode resonator–single-qutrit QBs and the resonator–multiple-qutrit QB. We investigate the performance of these QBs in the presence of the resonator decay and the qutrit decoherence and then discuss the roles of quantum entanglement and quantum coherence during their charging and self-discharging processes.

The paper is organized as follows. In Sec. II we derive the Hamiltonian of a superconducting circuit system and define a general QB model. In Sec. III we investigate the performance of the QB in the presence of the resonator decay and the qutrit decoherence. The roles of quantum entanglement and quantum coherence during their charging and self-discharging processes are discussed in Sec. IV. Finally, a brief conclusion is given in Sec. V.

II. MODEL AND HAMILTONIAN

A. The superconducting circuit system

The superconducting transmon is designed as a transmission-line-shunted plasma oscillation system, the favorable properties of which lie in the combination of the exponential decrease of the charge dispersion, the slow power-law decay of the anharmonicity, and the realization of strong coupling to the transmission line resonator [72–78]. Our previous work has proposed a superconducting circuit system based on a transmission line resonator and N transmons. In the small resonator-transmon detuning regime, we have derived the Hamiltonian of the resonator-qubits system only considering the lowest mode of the resonator [50]. However, when the transmon anharmonicity is small compared to the resonator-transmon detuning, the transitions between states $|m+1\rangle$ and $|m\rangle$ are almost equally likely to be excited by the resonator, causing non-negligible leakage to higher excited states [79–82]. In such a condition, we expect to derive a more general light-matter interaction model based on a superconducting circuit system.

The classical Hamiltonian of the superconducting circuit system, which consists of a one-dimensional transmission line resonator and N capacitively coupled transmons, is described by [50]

$$H^{\rm cl}=H_r^{\rm cl}-\sum_{i=1}^{N}C_c\dot{\Phi}_r\dot{\Phi}_i+\frac{1}{2}\vec{\dot{\Phi}}\mathcal{C}\vec{\dot{\Phi}}^T-\sum_{i=1}^{N}2E_J\cos\delta, \quad (1)$$

where $H_r^{\rm cl}$ is the classical Hamiltonian of the transmission line resonator, $\vec{\dot{\Phi}}=(\dot{\Phi}_1,\dot{\Phi}_2,\ldots,\dot{\Phi}_N)$ is the voltage vector, and $\dot{\Phi}_i(i=1,\ldots,N)$ and $\dot{\Phi}_r$ represent the voltage of the ith transmon and the resonator. E_J is the Josephson energy of each Josephson junction, δ is the phase difference between Josephson junctions constituting transmon, and the capacitance matrix $\mathcal{C}$ is given by

$$\mathcal{C}=\begin{bmatrix} C_0+C & -C & & & \\ -C & C_0+2C & -C & & \\ & -C & C_0+2C & -C & \\ & & -C & \ddots & \ddots \\ & & & \ddots & \end{bmatrix}.$$

Here, $C_0=2C_J+C_B+C_g+C_c$ and C_J, C_B, C_g, C_c, C_r, and C are capacitances in the superconducting circuit.

According to the quantization procedure of the transmon [83–85] and the transmission line resonator [78,86], we express

$$\begin{aligned}\vec{\Phi}^T&=2e\mathcal{C}^{-1}(\vec{n}-n_g)^T,\\ \dot{\Phi}_r&=\sum_k\sqrt{\hbar\omega_{rk}/(C_r+NC_c)}(a_k+a_k^\dagger),\end{aligned} \quad (2)$$

where $\vec{n}=(n_1,n_2,\ldots,n_N)$ is the vector of the Cooper pair number, n_i is the number of Cooper pairs transferred between Josephson junctions, and n_g is the number of gate charges. The quantized Hamiltonian of the resonator $H_r=\sum_k\hbar\omega_{rk}a_k^\dagger a_k$, with the frequency ω_{rk} and the creation (annihilation) operator $a_k^\dagger$ (a_k) of the kth harmonic oscillator constituting the resonator. Thus, the quantized Hamiltonian of the whole system can be written as

$$\begin{aligned}H=&\sum_k\hbar\omega_{rk}a_k^\dagger a_k+\sum_{i=1}^{N}\left[2e^2\mathcal{C}_{ii}^{-1}(n_i-n_g)^2-2E_J\cos\delta\right]\\&+\sum_{i<j}^{N}4e^2\mathcal{C}_{ij}^{-1}(n_i-n_g)(n_j-n_g)\\&-\frac{2eC_c}{C_0}\sum_k\sqrt{\frac{\hbar\omega_{rk}}{C_r+NC_c}}(a_k+a_k^\dagger)\sum_{i=1}^{N}(n_i-n_g).\end{aligned} \quad (3)$$

Defining $E_C=e^2/2C_0$, $\beta=C/(C_0+C)$ and substituting $\mathcal{C}_{ii}^{-1}\approx 1/C_0$, $\mathcal{C}_{ij}^{-1}\approx\beta^{|i-j|}/C_0$ into Eq. (3), the above Hamiltonian becomes

$$\begin{aligned}H=&\sum_k\hbar\omega_{rk}a_k^\dagger a_k+\sum_{i=1}^{N}[4E_C(n_i-n_g)^2-2E_J\cos\delta]\\&+\sum_{i<j}^{N}8E_C\beta^{|i-j|}(n_i-n_g)(n_j-n_g)\\&-\frac{2eC_c}{C_0}\sum_k\sqrt{\frac{\hbar\omega_{rk}}{C_r+NC_c}}(a_k+a_k^\dagger)\sum_{i=1}^{N}(n_i-n_g).\end{aligned} \quad (4)$$

It is noted that the Josephson energy E_J acts as a strong "gravitational force" on the rotor, effectively restricting the angle δ to small values around 0 [77]. This motivates the expansion of the cosine terms up to fourth order, and then the Hamiltonian can be expressed as

$$\begin{aligned}H=&\sum_k\hbar\omega_{rk}a_k^\dagger a_k+\sum_{i=1}^{N}\left[\omega_q b_i^\dagger b_i-\frac{E_C}{12}(b_i^\dagger+b_i)^4\right]\\&-\frac{\omega_q}{2}\sum_{i<j}\beta^{|i-j|}(b_i-b_i^\dagger)(b_j-b_j^\dagger)\\&+I\sum_k\sqrt{\frac{\omega_q\omega_{rk}E_CC_c^2}{e^2(C_r+NC_c)}}(a_k+a_k^\dagger)\sum_{i=1}^{N}(b_i-b_i^\dagger),\end{aligned} \quad (5)$$

where $b_i^\dagger$ (b_i) is the creation (annihilation) operator of the ith transmon, I represents the imaginary unit, $\delta=2\sqrt{E_C/\omega_q}$

$(b_i + b_i^\dagger)$, $n_i - n_g = -I\sqrt{\omega_q/E_C}(b_i - b_i^\dagger)/4$, and $\omega_q = \sqrt{16E_C E_J}$ is the frequency of the transmon.

In the following, we only consider the three lowest energy levels of the transmon since the main leakage out of the qubit basis comes from the third energy level [50,87,88]. The Hamiltonian (5) can be truncated to the three levels (including the ground state $|0\rangle$, the first excited state $|1\rangle$, and the second excited state $|2\rangle$) and written as

$$\begin{aligned} H =& \sum_k \hbar\omega_{rk} a_k^\dagger a_k + \sum_{i=1}^N S_i^z \\ &+ \frac{I^2\omega_q}{2}\sum_{i<j}\beta^{|i-j|}(S_i^- - S_i^+)(S_j^- - S_j^+) \\ &+ I\sum_k \sqrt{\frac{\omega_q\omega_{rk}E_C C_c^2}{e^2(C_r + NC_c)}}(a_k + a_k^\dagger)\sum_{i=1}^N (S_i^- - S_i^+), \end{aligned} \tag{6}$$

where the annihilation operator of the transmon b ($b \equiv |0\rangle\langle 1| + \sqrt{2}|1\rangle\langle 2| + \sqrt{3}|2\rangle\langle 3| + \cdots$ [89]) can be treated as $S_i^- = |0\rangle\langle 1| + \sqrt{2}|1\rangle\langle 2|$. $S_i^+ = |1\rangle\langle 0| + \sqrt{2}|2\rangle\langle 1|$, $S_i^z = \omega_0|0\rangle\langle 0| + \omega_1|1\rangle\langle 1| + \omega_2|2\rangle\langle 2|$, and ω_m is the frequency of the state $|m\rangle$. We ignore the long-range interaction, and the final quantized Hamiltonian of the resonator–multiple-qutrit system takes the following form:

$$\begin{aligned} H =& \sum_k \hbar\omega_{rk} a_k^\dagger a_k + \sum_{i=1}^N S_i^z + I^2 J\sum_{i=1}^{N-1}(S_i^- - S_i^+)(S_{i+1}^- - S_{i+1}^+) \\ &+ I\sum_k g_k(a_k + a_k^\dagger)\sum_{i=1}^N (S_i^- - S_i^+), \end{aligned} \tag{7}$$

where $\omega_{rk} = k\pi/\sqrt{L_r(C_r + NC_c)}$ is the frequency of the kth harmonic oscillator constituting the resonator, $J = \omega_q\beta/2$ is the nearest-neighbor interaction strength between the qutrits, and $g_k = \sqrt{\omega_q\omega_{rk}E_C C_c^2/[e^2(C_r + NC_c)]}$ is the resonator-single-qutrit coupling strength.

B. The resonator–multiple-qutrit QB model

For the convenience of numerical simulation, we consider that the transmon qutrits are coupled to the two modes ($k = 1$ and 2) of the transmission line resonator and the Hamiltonian of the resonator–multiple-qutrit system can be simplified to (hereafter we set $\hbar = 1$)

$$H = H_r + H_q + H_{r-q}, \tag{8}$$

where

$$\begin{aligned} H_r &= \omega_r\sum_{k=1}^2 a_k^\dagger a_k, \\ H_q &= \sum_{i=1}^N S_i^z + I^2 J\sum_{i=1}^{N-1}(S_i^- - S_i^+)(S_{i+1}^- - S_{i+1}^+), \\ H_{r-q} &= Ig\sum_{k=1}^2 (a_k + a_k^\dagger)\sum_{i=1}^N (S_i^- - S_i^+). \end{aligned} \tag{9}$$

Here we set $g = \sqrt{\omega_q\omega_r E_C C_c^2/[e^2(C_r + NC_c)]}$, with $\omega_r = 2\pi/\sqrt{L_r(C_r + NC_c)}$. H_r, H_q, and H_{r-q} are the Hamiltonian of the transmission line resonator, the transmon qutrits with nearest-neighbor interactions, and the resonator–multiple-qutrit coupling, respectively.

We define that the N capacitively coupled transmon qutrits H_q plays the role of the battery and the resonator H_r plays the role of the charger. In real scenarios, the QB systems are regarded as open systems due to the inevitable interactions with complex environments. Therefore, we mainly explore the charging and self-discharging performance of our QB with three relevant environmental effects.

When the resonator–multiple-qutrit coupling is switched on, the charging process immediately starts. The charging dynamics of the QB is described by the Lindblad master equation

$$\dot{\rho}_c(t) = I[\rho_c, H] + \mathbb{L}_a[\rho_c] + \mathbb{L}_{\rm rel}[\rho_c] + \mathbb{L}_{\rm dep}[\rho_c], \tag{10}$$

where the superoperators $\mathbb{L}_a[\bullet]$, $\mathbb{L}_{\rm rel}[\bullet]$, and $\mathbb{L}_{\rm dep}[\bullet]$ describe three relevant environmental effects including the resonator decay, the qutrit relaxation, and the qutrit dephasing processes, respectively. $\mathbb{L}_a[\bullet]$, $\mathbb{L}_{\rm rel}[\bullet]$, and $\mathbb{L}_{\rm dep}[\bullet]$ can be written as

$$\begin{aligned} \mathbb{L}_a[\bullet] &= \sum_{k=1}^2 \kappa\left[a_k \bullet a_k^\dagger - \frac{1}{2}\{a_k^\dagger a_k, \bullet\}\right], \\ \mathbb{L}_{\rm rel}[\bullet] &= \sum_{m=1,2}\Gamma_{nm}\left[S_{nm}\bullet S_{mn} - \frac{1}{2}\{S_{mm}, \bullet\}\right], \\ \mathbb{L}_{\rm dep}[\bullet] &= \sum_{m=1,2}\Gamma_{mm}\left[S_{mm}\bullet S_{mm} - \frac{1}{2}\{S_{mm}, \bullet\}\right]. \end{aligned} \tag{11}$$

In the above superoperators, $S_{mn} = \sum_{i=1}^N \sigma_i^{mn}$, $\sigma_i^{mn} = |m\rangle\langle n|$, $n = m - 1$ ($m = 1$ and 2), and $\rho_c(t) = |\psi_c(t)\rangle\langle\psi_c(t)|$ is the density matrix of the QB system during the charging process. These three relevant environmental effects correspond to the resonator decay rate κ, the qutrit relaxation rates Γ_{01} and Γ_{12}, and the qutrit dephasing rates Γ_{11} and Γ_{22}, respectively.

We prepared the initial state of the battery and the charger in the ground state $|G\rangle = |0\rangle^{\otimes N}$ and the Fock state $|n_{r1}\rangle \otimes |n_{r2}\rangle$. Thus, the initial state of the QB system during the charging process is as follows:

$$|\psi_c(0)\rangle = |G\rangle \otimes |n_{r1}\rangle \otimes |n_{r2}\rangle. \tag{12}$$

The energy in the battery can be defined in terms of the mean of the Hamiltonian H_q at time t, i.e.,

$$E_c(t) = {\rm Tr}[H_q\rho_q(t)], \tag{13}$$

where $\rho_q(t) = {\rm Tr}_r[\rho_c(t)]$ is the reduced density matrix of the battery. The stored energy is the difference of energy between the final and initial battery states:

$$\Delta E_c(t) = E_c(t) - E_c(0), \tag{14}$$

where $E_c(0) = 0$ is the ground-state energy of the battery. The average charging power is defined as

$$P_c(t) = \Delta E_c(t)/t. \tag{15}$$

In addition to the stored energy ΔE_c and the average charging power P_c, equally important is assessing the stable energy E_s and the maximum power $P_{\max}$ of the QB, which can be quantified as

$$E_s = \Delta E_c(\infty), \quad P_{\max} = \max[P_c(t)]. \tag{16}$$

For open systems, the logarithmic negativity provides a convenient measure of entanglement [16,90]. The entanglement between the charger and the battery is defined by the trace norm as

$$S_c(t) = \log_2 \|\rho_q(t)\|. \tag{17}$$

One of the most common measures of coherence for quantum states is the l_1 norm of coherence measuring the overall magnitude of off-diagonal elements [91,92], which we express as

$$C_c(t) = \sum_{i \neq j} |\rho_q(t)|. \tag{18}$$

When the battery is disconnected from the charger and any consumption hub, the resonator–multiple-qutrit QB begins to self-discharge due to the inevitable interaction between the qutrits and the environment. Here we consider the qutrit decoherence process (a combination of the relaxation and the dephasing process), the self-discharging dynamics of the QB is obtained by solving the following equation:

$$\dot{\rho_d}(t) = I[\rho_d, H_q] + \mathbb{L}_{\text{rel}}[\rho_d] + \mathbb{L}_{\text{dep}}[\rho_d]. \tag{19}$$

The forms of the superoperators $\mathbb{L}_{\text{rel}}[\bullet]$ and $\mathbb{L}_{\text{dep}}[\bullet]$ are shown in Eq. (11), and $\rho_d(t)$ is the density matrix of the QB system during the self-discharging process.

We assume that the initial state of the battery $\rho_d(0)$ in the self-discharging process is the final state of the battery in the charging process. The energy at time t reads

$$E_d(t) = \text{Tr}[H_q \rho_d(t)], \tag{20}$$

and the l_1 norm of coherence during the self-discharging process is

$$C_d(t) = \sum_{i \neq j} |\rho_d(t)|. \tag{21}$$

III. THE CHARGING AND SELF-DISCHARGING PROPERTIES

In this section, we investigate the charging and self-discharging performance of the QB under three environmental effects. We mainly consider the resonance regime of the transition frequency between the resonator and the qutrit ($|0\rangle \leftrightarrow |1\rangle$) unless mentioned otherwise, i.e., $\omega_r = \omega_1 - \omega_0 = \omega$ in Eq. (9). For simplicity of calculation, we take that all physical quantities are in units of ω and set $\omega = 1$, $\omega_0 = 0, \omega_1 = 1, \omega_2 = 1.95, n_{r1} = n_{r2} = 2N, \Gamma_{12} = 2\Gamma_{01}$, and $\Gamma_{22} = 2\Gamma_{11}$.

A. The stable charging with resonator decay and qutrit decoherence

In the following, we focus on the charging performance of three QBs defined by Eq. (9), including one-mode and two-mode single-cell QBs and one-mode many-body QBs. The two single-cell QBs are defined as resonator–single-qutrit QBs consisting of a qutrit and a one-mode or two-mode resonator. In order to evaluate whether the single-cell QBs have charging advantages over existing QBs based on superconducting circuits, we also discuss the qutrit QB [54], which consists of a qutrit driven by two classical fields. The Hamiltonian of the qutrit QB is defined by

$$H_{\text{qutrit}} = H_0 + H_t, \tag{22}$$

where

$$\begin{aligned} H_0 &= \omega_0|0\rangle\langle 0| + \omega_1|1\rangle\langle 1| + \omega_2|2\rangle\langle 2|, \\ H_t &= \Omega_{01}e^{-I\omega_{01}t}|0\rangle\langle 1| + \Omega_{12}e^{-I\omega_{12}t}|1\rangle\langle 2| + \text{H.c.} \end{aligned} \tag{23}$$

Here $\omega_{mn} = \omega_n - \omega_m$ $(m, n = 0, 1, 2)$ is the transition frequency from states $|m\rangle$ to $|n\rangle$. $\Omega_{01}(t) = \Omega_0 f(t)$ and $\Omega_{12}(t) = \Omega_0[1 - f(t)]$ are two classical fields, Ω_0 is a parameter related to the amplitude of two fields, and the function $f(t) = t/\tau$ satisfies $f(0) = 0$ and $f(\tau) = 1$.

The stored energy $\Delta E_c(t)$ of the qutrit QB and the resonator–single-qutrit QBs over the evolution time are shown in Figs. 1(a)–1(d). In closed systems, the stored energy of the resonator–single-qutrit QBs is unstable and highly oscillatory. However, the qutrit QB using stimulated Raman adiabatic passage suppresses the nonadiabatic excitation during the charging process, thus achieving a QB with stable and higher energy storage. In open systems, the quantum interference inhibits the highly oscillatory phenomenon and results in the resonator–single-qutrit QBs eventually reaching steady states (subradiant states) [93–95]. Comparing the red and green curves in Figs. 1(a)–1(c), we find that the stable energy of the resonator–single-qutrit QBs is higher and this advantage still exists when considering the resonator decay of the resonator–single-qutrit QBs [see cases $\kappa \neq 0$ in Fig. 1(d)]. The time evolutions of the average charging power $P_c(t)$ in these single-cell QBs are described by Figs. 1(e)–1(h). It is worth noting that the average charging power of the resonator–single-qutrit QBs is always significantly higher than that of the qutrit QB, regardless of whether open systems are taken into account. In particular, the average charging power of the resonator–single-qutrit QB is the highest when the two-mode resonator is used as a charger. This indicates that the resonator–single-qutrit QBs have charging processes that are more efficient than those of the qutrit QB, and the multiplied increasing photons in the two-mode resonator–single-qutrit QB leads to an acceleration mechanism of its charging process.

Although the stable energy of the resonator–single-qutrit QB is higher compared to that of the qutrit QB, its stored energy is still very limited. Next we discuss the charging performance of the resonator–multiple-qutrit QB, namely, the many-body QB, which consists of a one-mode resonator and N coupled qutrits. As shown in Fig. 2, the stored energy $\Delta E_c(t)$ and the average charging power $P_c(t)$ of the resonator–multiple-qutrit QB can be obtained by solving Eq. (10). By utilizing subradiant states to tune qutrits into a decoherence-free subspace [96–98], the resonator–multiple-qutrit QB also has a stable charging process when considering the resonator decay and the qutrit decoherence. In addition, Fig. 2 also indicates that the resonator decay has a positive effect on the stable and efficient charging of the resonator–multiple-qutrit QB, while the qutrit relaxation suppresses the population inversion

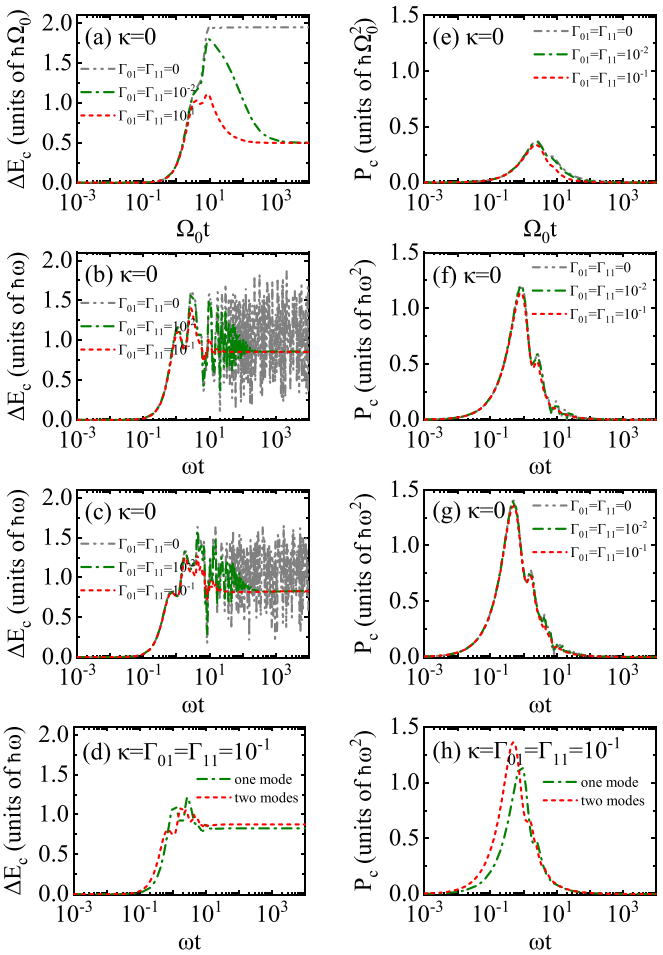

FIG. 1. (a)–(d) The time evolution of the stored energy $\Delta E_c(t)$ (units of $\hbar\Omega_0$ and $\hbar\omega$) and (e)–(h) the average charging power $P_c(t)$ (units of $\hbar\Omega_0^2$ and $\hbar\omega^2$) in single-cell QBs with qutrit relaxation and dephasing, where panels (a) and (e) describe the qutrit QB, and panels (b)–(d) and panels (f)–(h) describe the one-mode and two-mode resonator–single-qutrit QBs without and with resonator decay. The gray dash-dotted curve corresponds to the closed-system case, whereas other curves correspond to the open-system cases. The parameters are chosen as $N = 1$, $J = 0$, and $g = 1$.

between quantum states [77,99], which leads to a remarkable decay on the stable energy and the maximum charging power of the resonator–multiple-qutrit QB. The stable energy and the maximum charging power with decay rate in Fig. 3 verify this conclusion. It is also observed that compared to the resonator decay and the qutrit relaxation, the stable energy of the resonator–multiple-qutrit QB is higher and has good robustness when considering the qutrit dephasing. This is because the qutrit dephasing causes transitions between superradiant and subradiant states that suppress the emission of photons into the environment. Meanwhile, compared with our previous work [50], we find that the resonator–multiple-qutrit QB can store higher energy and charge faster than the resonator–multiple-qutrit QB, although two QBs both have efficient charging and stable energy-storage processes when considering the cases of open systems. The result demonstrates that the energy leakage to the second excited state can boost the performance of our QB.

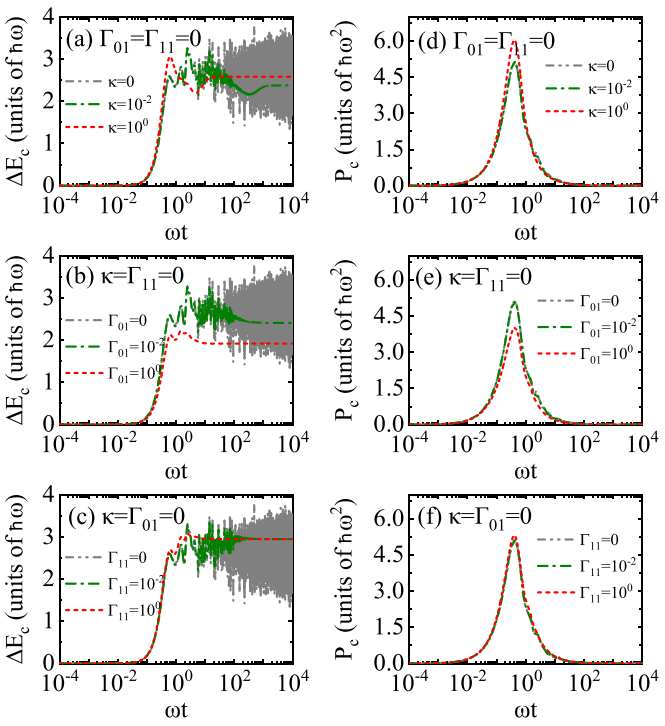

FIG. 2. (a)–(c) The time evolution of the stored energy $\Delta E_c(t)$ (units of $\hbar\omega$) and (d)–(f) the average charging power $P_c(t)$ (units of $\hbar\omega^2$) in many-body QB. The parameters are chosen as $N = 3$ and $J = g = 1$.

B. The slow self-discharging with qutrit decoherence

Similar to classical batteries, QBs also have a phenomenon known as the self-discharging process, which features the decay of energy stored in the battery even when no consumption hubs are coupled to them [54,56–58,100]. The self-discharging process is associated with the unwanted effects that deteriorate the energy-storage performance of the battery [56]. Next, we mainly explore how to reduce the speed

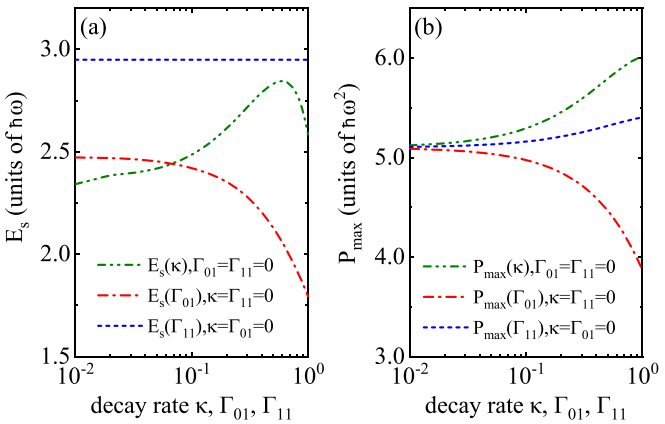

FIG. 3. The stable energy E_s (in units of $\hbar\omega$) and the maximum charging power $P_{\max}$ (in units of $\hbar\omega^2$) as a function of the decay rate (the resonator decay rate κ, the qutrit relaxation rate Γ_{01}, and the qutrit dephasing rate Γ_{11}). The other parameters are the same as those in Fig. 2.

of the self-discharging process of the resonator–multiple-qutrit QB.

We first consider the case of $N = 1$ in Eq. (19) and express its Hamiltonian and density matrix during the self-discharging process as

$$H_q = \begin{bmatrix} \omega_0 & 0 & 0 \\ 0 & \omega_1 & 0 \\ 0 & 0 & \omega_2 \end{bmatrix}, \quad \rho_d = \begin{bmatrix} \rho_{11} & \rho_{12} & \rho_{13} \\ \rho_{21} & \rho_{22} & \rho_{23} \\ \rho_{31} & \rho_{32} & \rho_{33} \end{bmatrix}.$$

The energy defined in Eq. (20) can be rewritten as

$$E_d(t) = \omega_0\rho_{11}(t) + \omega_1\rho_{22}(t) + \omega_2\rho_{33}(t). \tag{24}$$

Since $E_d(t)$ depends only on the diagonal element of the density matrix ρ_d, the task of finding the analytic solution of $E_d(t)$ reduces to the problem of solving the following equations:

$$\begin{aligned} \dot{\rho_{11}}(t) &= \Gamma_{01}\rho_{22}(t), \\ \dot{\rho_{22}}(t) &= -\Gamma_{01}\rho_{22}(t) + \Gamma_{12}\rho_{33}(t), \\ \dot{\rho_{33}}(t) &= -\Gamma_{12}\rho_{33}(t), \end{aligned} \tag{25}$$

whose solutions are as follows:

$$\begin{aligned} \rho_{11}(t) &= \frac{\Gamma_{12}e^{-\Gamma_{01}t} - \Gamma_{01}e^{-\Gamma_{12}t}}{\Gamma_{01} - \Gamma_{12}} + 1, \\ \rho_{22}(t) &= \frac{\Gamma_{12}e^{-\Gamma_{12}t} - \Gamma_{12}e^{-\Gamma_{01}t}}{\Gamma_{01} - \Gamma_{12}}, \\ \rho_{33}(t) &= e^{-\Gamma_{12}t}, \end{aligned} \tag{26}$$

where we assume the initial state of the battery during the self-discharging process in its second excited state $|2\rangle$ and use the normalization condition $\rho_{11}(t) + \rho_{22}(t) + \rho_{33}(t) = 1$. The analytic solution of the energy during the self-discharging process is as follows:

$$E_d(t) = \frac{e^{-\Gamma_{12}t}(\Gamma_{01}\omega_{02} - \Gamma_{12}\omega_{12}) - e^{-\Gamma_{01}t}\Gamma_{12}\omega_{01}}{\Gamma_{01} - \Gamma_{12}} + \omega_0. \tag{27}$$

For the single-cell QB, Eq. (27) reveals that the energy during the self-discharging process is only affected by the energy gap and the relaxation rate, not related to the dephasing rate. However, for the resonator–multiple-qutrit QB, due to the presence of nearest-neighbor interaction terms between qutrits, the dephasing process inevitably affects its self-discharging process. Therefore, we fix the relaxation rate and focus on the effects of the dephasing rate and the energy gap on the energy during the self-discharging process of the resonator–multiple-qutrit QB, as shown in Fig. 4. It is obvious that the energy stored in the resonator–multiple-qutrit QB increases and the self-discharging speed decreases with the increase of the dephasing rate and the relative energy gap. This means that we can realize a longer-lived QB with both an efficient charging process and a slow self-discharging process by considering the dephasing process and manipulating the energy gap.

IV. THE ROLES OF QUANTUM ENTANGLEMENT AND QUANTUM COHERENCE

As the QB charges superextensively, it will also discharge superextensively if the battery is simply disconnected from the charger [16]. However, our resonator–multiple-qutrit QB has both an efficient charging process and a slow self-discharging process. This is because we propose a dephasing process before disconnecting the charger. In this section, in order to find out how the dephasing process specifically determines the behavior of the energy in the resonator–multiple-qutrit QB, we introduce coherence and entanglement, characterized by the l_1 norm of the off-diagonal elements and the logarithmic negativity, respectively.

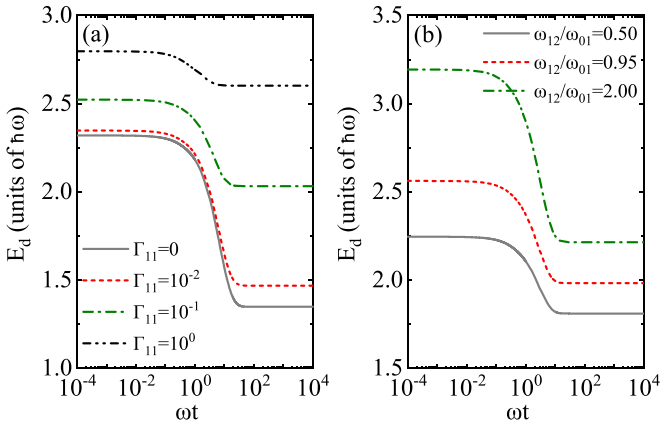

FIG. 4. The time evolution of the energy $E_d(t)$ (units of $\hbar\omega$) in the self-discharging process of the resonator–multiple-qutrit QB for different choices of the dephasing rate Γ_{11} and the energy gap ω_{12}/ω_{01}. The parameters are fixed as $N = 3$, $g = J = 1$, and $\kappa = \Gamma_{01} = 10^{-1}$.

In Fig. 5, we illustrate the evolutions of entanglement and coherence for different dephasing rates. Before the maximum energy is reached during the charging process, note that if there is no battery coherence and no battery-charger entanglement, then the energy of the resonator–multiple-qutrit QB is always 0. This means the energy is positively related to

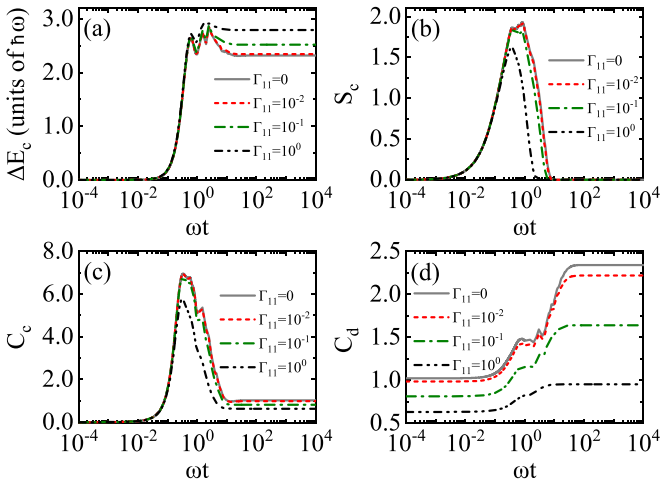

FIG. 5. (a), (b) Entanglement and energy. The time evolution of the stored energy $\Delta E_c(t)$ (units of $\hbar\omega$) and the logarithmic negativity S_c during the charging process of the resonator–multiple-qutrit QB. (c), (d) Coherence. The time evolution of the l_1 coherence $C_c(t)$, $C_d(t)$ during the charging and self-discharging processes of the resonator–multiple-qutrit QB. The other parameters are the same as those in Fig. 4.

coherence and entanglement and further demonstrates that the coherence in the battery or the entanglement between the battery and the charger is a necessary resource for generating nonzero energy during the charging process. At the end of the charging process, we can establish a tight link of coherence and entanglement with the stable energy: (i) The relationship between coherence and energy shows that lower coherence corresponds to higher steady-state energy, meaning that the coherence in the battery inhibits the stable energy of the resonator–multiple-qutrit QB. (ii) The phenomenon of the battery-charger entanglement suddenly disappearing when the battery reaches steady states just verifies the physical mechanism of steady-state generation, that is, the dynamic decoupling behavior due to the quantum interference caused by the collective effects between the QB and the environment. In addition, during the whole self-discharging process, it is worth mentioning that the increasing coherence causes the battery to discharge at a superradiant decay rate and has a detrimental effect on the energy, as shown in Fig. 4(a) and Fig. 5(d). Thus, our results suggest that the dephasing process, which destroys the coherence of the battery in its energy eigenbasis, shows a counterintuitive advantage in the self-discharging process of the resonator–multiple-qutrit QB.

V. CONCLUSIONS

In this work, we have derived the Hamiltonian of a light-matter interaction model based on a superconducting circuit platform and we have defined three QBs. We have investigated the charging performance of these QBs in the presence of the resonator decay and the qutrit decoherence. Our results have shown that, for the single-cell case, the one-mode or two-mode resonator–single-qutrit QBs have both higher stable energy and charging power than existing QBs based on superconducting circuits. For the many-body case, we have achieved a resonator–multiple-qutrit QB with a stable and efficient charging process by utilizing subradiant states to tune qutrits into a decoherence-free subspace. Meanwhile, we have explored how to reduce the speed of the self-discharging process of the resonator–multiple-qutrit QB. Our findings suggest that the resonator–multiple-qutrit QB with a slow self-discharging process can be realized by considering the dephasing process and manipulating the energy gap. Remarkably, we have also emphasized the necessity of battery coherence and battery-charger entanglement for generating nonzero energy of the resonator–multiple-qutrit QB. The charging energy is positively related to coherence and entanglement while the stable energy and the self-discharging energy are negatively related to coherence. The phenomenon of entanglement suddenly disappearing when the battery reaches steady states corresponds to the dynamic decoupling behavior caused by quantum interference. Our QBs address inadequacies of the previously proposed QBs based on superconducting circuit systems [69–71]. The results provide an alternative way for further realization of many-body QBs with efficient charging, stable energy-storage, and slow self-discharging processes on a superconducting circuit platform.

ACKNOWLEDGMENT

The work is supported by the National Natural Science Foundation of China (Grant No. 12075193).

[1] R. Alicki and M. Fannes, Phys. Rev. E **87**, 042123 (2013).
[2] K. V. Hovhannisyan, M. Perarnau-Llobet, M. Huber, and A. Acín, Phys. Rev. Lett. **111**, 240401 (2013).
[3] G. L. Giorgi and S. Campbell, J. Phys. B: At., Mol. Opt. Phys. **48**, 035501 (2015).
[4] J.-X. Liu, H.-L. Shi, Y.-H. Shi, X.-H. Wang, and W.-L. Yang, Phys. Rev. B **104**, 245418 (2021).
[5] G. M. Andolina, M. Keck, A. Mari, M. Campisi, V. Giovannetti, and M. Polini, Phys. Rev. Lett. **122**, 047702 (2019).
[6] J.-Y. Gyhm and U. R. Fischer, AVS Quantum Sci. **6**, 012001 (2024).
[7] H.-L. Shi, S. Ding, Q.-K. Wan, X.-H. Wang, and W.-L. Yang, Phys. Rev. Lett. **129**, 130602 (2022).
[8] F. H. Kamin, F. T. Tabesh, S. Salimi, and A. C. Santos, Phys. Rev. E **102**, 052109 (2020).
[9] B. Çakmak, Phys. Rev. E **102**, 042111 (2020).
[10] M. Gumberidze, M. Kolář, and R. Filip, Sci. Rep. **9**, 19628 (2019).
[11] L. P. García-Pintos, A. Hamma, and A. del Campo, Phys. Rev. Lett. **125**, 040601 (2020).
[12] C. L. Latune, I. Sinayskiy, and F. Petruccione, Phys. Rev. A **99**, 052105 (2019).
[13] F. Mayo and A. J. Roncaglia, Phys. Rev. A **105**, 062203 (2022).
[14] S. Seah, M. Perarnau-Llobet, G. Haack, N. Brunner, and S. Nimmrichter, Phys. Rev. Lett. **127**, 100601 (2021).
[15] K. Sen and U. Sen, Phys. Rev. A **104**, L030402 (2021).
[16] J. Q. Quach and W. J. Munro, Phys. Rev. Appl. **14**, 024092 (2020).
[17] J.-Y. Gyhm, D. Šafránek, and D. Rosa, Phys. Rev. Lett. **128**, 140501 (2022).
[18] J. Goold, M. Huber, A. Riera, L. D. Rio, and P. Skrzypczyk, J. Phys. A: Math. Theor. **49**, 143001 (2016).
[19] J. Millen and A. Xuereb, New J. Phys. **18**, 011002 (2016).
[20] F. Campaioli, F. A. Pollock, F. C. Binder, L. Céleri, J. Goold, S. Vinjanampathy, and K. Modi, Phys. Rev. Lett. **118**, 150601 (2017).
[21] Y. Guryanova, S. Popescu, A. J. Short, R. Silva, and P. Skrzypczyk, Nat. Commun. **7**, 12049 (2016).
[22] D. Rossini, G. M. Andolina, D. Rosa, M. Carrega, and M. Polini, Phys. Rev. Lett. **125**, 236402 (2020).
[23] A. Crescente, M. Carrega, M. Sassetti, and D. Ferraro, New J. Phys. **22**, 063057 (2020).
[24] T. P. Le, J. Levinsen, K. Modi, M. M. Parish, and F. A. Pollock, Phys. Rev. A **97**, 022106 (2018).
[25] T. K. Konar, L. G. C. Lakkaraju, S. Ghosh, and A. Sen(De), Phys. Rev. A **106**, 022618 (2022).
[26] V. Shaghaghi, V. Singh, G. Benenti, and D. Rosa, Quantum Sci. Technol. **7**, 04LT01 (2022).
[27] R. R. Rodríguez, B. Ahmadi, P. Mazurek, S. Barzanjeh, R. Alicki, and P. Horodecki, Phys. Rev. A **107**, 042419 (2023).
[28] F. Mazzoncini, V. Cavina, G. M. Andolina, P. A. Erdman, and V. Giovannetti, Phys. Rev. A **107**, 032218 (2023).

[29] S.-Y. Bai and J.-H. An, Phys. Rev. A **102**, 060201(R) (2020).

[30] W.-L. Song, H.-B. Liu, B. Zhou, W.-L. Yang, and J.-H. An, Phys. Rev. Lett. **132**, 090401 (2024).

[31] G. M. Andolina, D. Farina, A. Mari, V. Pellegrini, V. Giovannetti, and M. Polini, Phys. Rev. B **98**, 205423 (2018).

[32] A. Crescente, M. Carrega, M. Sassetti, and D. Ferraro, Phys. Rev. B **102**, 245407 (2020).

[33] D. Ferraro, M. Campisi, G. M. Andolina, V. Pellegrini, and M. Polini, Phys. Rev. Lett. **120**, 117702 (2018).

[34] F. Barra, Phys. Rev. Lett. **122**, 210601 (2019).

[35] Y. V. de Almeida, T. F. F. Santos, and M. F. Santos, Phys. Rev. A **108**, 052218 (2023).

[36] A. Crescente, D. Ferraro, M. Carrega, and M. Sassetti, Entropy **25**, 758 (2023).

[37] G. Gemme, G. M. Andolina, F. M. Pellegrino, M. Sassetti, and D. Ferraro, Batteries **9**, 197 (2023).

[38] F.-Q. Dou, Y.-Q. Lu, Y.-J. Wang, and J.-A. Sun, Phys. Rev. B **105**, 115405 (2022).

[39] F.-Q. Dou, H. Zhou, and J.-A. Sun, Phys. Rev. A **106**, 032212 (2022).

[40] F. Zhao, F.-Q. Dou, and Q. Zhao, Phys. Rev. Res. **4**, 013172 (2022).

[41] D.-L. Yang, F.-M. Yang, and F.-Q. Dou, arXiv:2308.01188.

[42] W.-X. Guo, F.-M. Yang, and F.-Q. Dou, Phys. Rev. A **109**, 032201 (2024).

[43] A. C. Santos, A. Saguia, and M. S. Sarandy, Phys. Rev. E **101**, 062114 (2020).

[44] S. Gherardini, F. Campaioli, F. Caruso, and F. C. Binder, Phys. Rev. Res. **2**, 013095 (2020).

[45] L. F. C. Moraes, A. Saguia, A. C. Santos, and M. S. Sarandy, Europhys. Lett. **136**, 23001 (2021).

[46] D. Rosa, D. Rossini, G. M. Andolina, M. Polini, and M. Carrega, J. High Energy Phys. 11 (2020) 067.

[47] Y. Yao and X. Q. Shao, Phys. Rev. E **104**, 044116 (2021).

[48] C. Rodríguez, D. Rosa, and J. Olle, Phys. Rev. A **108**, 042618 (2023).

[49] F. Zhao, F.-Q. Dou, and Q. Zhao, Phys. Rev. A **103**, 033715 (2021).

[50] F.-Q. Dou and F.-M. Yang, Phys. Rev. A **107**, 023725 (2023).

[51] F.-Q. Dou, Y.-J. Wang, and J.-A. Sun, Europhys. Lett. **131**, 43001 (2020).

[52] F.-Q. Dou, Y.-J. Wang, and J.-A. Sun, Front. Phys. **17**, 31503 (2022).

[53] M. Hadipour, S. Haseli, and S. Haddadi, arXiv:2312.06389.

[54] A. C. Santos, B. Çakmak, S. Campbell, and N. T. Zinner, Phys. Rev. E **100**, 032107 (2019).

[55] A. G. Catalano, S. M. Giampaolo, O. Morsch, V. Giovannetti, and F. Franchini, arXiv:2307.02529.

[56] F. H. Kamin, F. T. Tabesh, S. Salimi, F. Kheirandish, and A. C. Santos, New J. Phys. **22**, 083007 (2020).

[57] A. C. Santos, Phys. Rev. E **103**, 042118 (2021).

[58] M. B. Arjmandi, H. Mohammadi, and A. C. Santos, Phys. Rev. E **105**, 054115 (2022).

[59] F. Metzler, J. I. Sandoval, and N. Galvanetto, J. Phys. Energy **5**, 041001 (2023).

[60] J. Q. Quach, K. E. McGhee, L. Ganzer, D. M. Rouse, B. W. Lovett, E. M. Gauger, J. Keeling, G. Cerullo, D. G. Lidzey, and T. Virgili, Sci. Adv. **8**, eabk3160 (2022).

[61] J. Monsel, M. Fellous-Asiani, B. Huard, and A. Auffèves, Phys. Rev. Lett. **124**, 130601 (2020).

[62] C. Cruz, M. F. Anka, M. S. Reis, R. Bachelard, and A. C. Santos, Quantum Sci. Technol. **7**, 025020 (2022).

[63] G. Gemme, M. Grossi, D. Ferraro, S. Vallecorsa, and M. Sassetti, Batteries **8**, 43 (2022).

[64] G. Gemme, M. Grossi, S. Vallecorsa, M. Sassetti, and D. Ferraro, Phys. Rev. Res. **6**, 023091 (2024).

[65] J. Joshi and T. S. Mahesh, Phys. Rev. A **106**, 042601 (2022).

[66] I. Wenniger, S. Thomas, M. Maffei, S. Wein, M. Pont, A. Harouri, A. Lemaître, I. Sagnes, N. Somaschi, A. Auffèves *et al.*, arXiv:2202.01109.

[67] X. Huang, K. Wang, L. Xiao, L. Gao, H. Lin, and P. Xue, Phys. Rev. A **107**, L030201 (2023).

[68] G. Zhu, Y. Chen, Y. Hasegawa, and P. Xue, Phys. Rev. Lett. **131**, 240401 (2023).

[69] C.-K. Hu, J. Qiu, P. J. P. Souza, J. Yuan, Y. Zhou, L. Zhang, J. Chu, X. Pan, L. Hu, J. Li, Y. Xu, Y. Zhong, S. Liu, F. Yan, D. Tan, R. Bachelard, C. J. Villas-Boas, A. C. Santos, and D. Yu, Quantum Sci. Technol. **7**, 045018 (2022).

[70] R.-H. Zheng, W. Ning, Z.-B. Yang, Y. Xia, and S.-B. Zheng, New J. Phys. **24**, 063031 (2022).

[71] Y.-Y. Ge, X.-M. Yu, W. Xin, Z.-M. Wang, Y. Zhang, W. Zheng, S.-X. Li, D. Lan, and Y. Yu, Appl. Phys. Lett. **123**, 154002 (2023).

[72] J. Q. You and F. Nori, Phys. Today **58**(11), 42 (2005).

[73] M. H. Devoret and R. J. Schoelkopf, Science **339**, 1169 (2013).

[74] Z.-L. Xiang, S. Ashhab, J. Q. You, and F. Nori, Rev. Mod. Phys. **85**, 623 (2013).

[75] X. Gu, A. F. Kockum, A. Miranowicz, Y.-X. Liu, and F. Nori, Phys. Rep. **718-719**, 1 (2017).

[76] Y. Y. Gao, M. A. Rol, S. Touzard, and C. Wang, PRX Quantum **2**, 040202 (2021).

[77] J. Koch, T. M. Yu, J. Gambetta, A. A. Houck, D. I. Schuster, J. Majer, A. Blais, M. H. Devoret, S. M. Girvin, and R. J. Schoelkopf, Phys. Rev. A **76**, 042319 (2007).

[78] A. Blais, A. L. Grimsmo, S. M. Girvin, and A. Wallraff, Rev. Mod. Phys. **93**, 025005 (2021).

[79] J. Bourassa, F. Beaudoin, J. M. Gambetta, and A. Blais, Phys. Rev. A **86**, 013814 (2012).

[80] R. Schutjens, F. A. Dagga, D. J. Egger, and F. K. Wilhelm, Phys. Rev. A **88**, 052330 (2013).

[81] M. J. Peterer, S. J. Bader, X. Jin, F. Yan, A. Kamal, T. J. Gudmundsen, P. J. Leek, T. P. Orlando, W. D. Oliver, and S. Gustavsson, Phys. Rev. Lett. **114**, 010501 (2015).

[82] J.-M. Pirkkalainen, S. U. Cho, J. Li, G. S. Paraoanu, P. J. Hakonen, and M. A. Sillanpää, Nature (London) **494**, 211 (2013).

[83] K. Masuki, H. Sudo, M. Oshikawa, and Y. Ashida, Phys. Rev. Lett. **129**, 087001 (2022).

[84] T. Jaako, Z.-L. Xiang, J. J. Garcia-Ripoll, and P. Rabl, Phys. Rev. A **94**, 033850 (2016).

[85] K. Kaur, T. Sépulcre, N. Roch, I. Snyman, S. Florens, and S. Bera, Phys. Rev. Lett. **127**, 237702 (2021).

[86] A. Blais, R.-S. Huang, A. Wallraff, S. M. Girvin, and R. J. Schoelkopf, Phys. Rev. A **69**, 062320 (2004).

[87] K. Juliusson, S. Bernon, X. Zhou, V. Schmitt, H. le Sueur, P. Bertet, D. Vion, M. Mirrahimi, P. Rouchon, and D. Esteve, Phys. Rev. A **94**, 063861 (2016).

[88] T. Chen, J. Zhang, and Z.-Y. Xue, Phys. Rev. A **98**, 052314 (2018).
[89] S. Zeytinoğlu, M. Pechal, S. Berger, A. A. Abdumalikov, A. Wallraff, and S. Filipp, Phys. Rev. A **91**, 043846 (2015).
[90] L. Amico, R. Fazio, A. Osterloh, and V. Vedral, Rev. Mod. Phys. **80**, 517 (2008).
[91] T. Baumgratz, M. Cramer, and M. B. Plenio, Phys. Rev. Lett. **113**, 140401 (2014).
[92] X. Yang, Y.-H. Yang, M. Alimuddin, R. Salvia, S.-M. Fei, L.-M. Zhao, S. Nimmrichter, and M.-X. Luo, Phys. Rev. Lett. **131**, 030402 (2023).
[93] A. Albrecht, L. Henriet, A. Asenjo-Garcia, P. B. Dieterle, O. Painter, and D. E. Chang, New J. Phys. **21**, 025003 (2019).
[94] Z. Wang, H. Li, W. Feng, X. Song, C. Song, W. Liu, Q. Guo, X. Zhang, H. Dong, D. Zheng, H. Wang, and D.-W. Wang, Phys. Rev. Lett. **124**, 013601 (2020).
[95] M. Zanner, T. Orell, C. M. F. Schneider, R. Albert, S. Oleschko, M. L. Juan, M. Silveri, and G. Kirchmair, Nat. Phys. **18**, 538 (2022).
[96] D. A. Lidar, I. L. Chuang, and K. B. Whaley, Phys. Rev. Lett. **81**, 2594 (1998).
[97] P. G. Kwiat, A. J. Berglund, J. B. Altepeter, and A. G. White, Science **290**, 498 (2000).
[98] A. F. Kockum, G. Johansson, and F. Nori, Phys. Rev. Lett. **120**, 140404 (2018).
[99] P. Krantz, M. Kjaergaard, F. Yan, T. P. Orlando, S. Gustavsson, and W. D. Oliver, Appl. Phys. Rev. **6**, 021318 (2019).
[100] B. Mohan and A. K. Pati, Phys. Rev. A **104**, 042209 (2021).